The American Journal of Pathology, Vol. 173, No. 5, November 2008

DOI: 10.2353/ajpath.2008.080466

Cell Injury, Repair, Aging and Apoptosis

Inhibition of Nuclear Translocation of Apoptosis-Inducing Factor Is an Essential Mechanism of the Neuroprotective Activity of Pigment Epithelium-Derived Factor in a Rat Model of Retinal Degeneration

Yusuke Murakami,*† Yasuhiro Ikeda,† Yoshikazu Yonemitsu,‡ Mitsuho Onimaru,* Kazunori Nakagawa,* Ri-ichiro Kohno,† Masanori Miyazaki,† Toshio Hisatomi,† Makoto Nakamura,§ Takeshi Yabe,¶ Mamoru Hasegawa,‖ Tatsuro Ishibashi,† and Katsuo Sueishi*

From the Department of Pathology, Division of Pathophysiological and Experimental Pathology, and the Department of Ophthalmology,† Graduate School of Medical Sciences, Kyushu University, Fukuoka; the Department of Gene Therapy,‡ Chiba University Graduate School of Medicine, Chiba; the Department of Organs Therapeutics,§ Division of Ophthalmology, Kobe University Graduate School of Medicine, Kobe; the Kitasato Institute for Life Sciences,¶ Kitasato University, Tokyo; and DNAVEC Corporation,‖ Ibaraki, Japan*

Photoreceptor apoptosis is a critical process of retinal degeneration in retinitis pigmentosa (RP), a group of retinal degenerative diseases that result from rod and cone photoreceptor cell death and represent a major cause of adult blindness. We previously demonstrated the efficient prevention of photoreceptor apoptosis by intraocular gene transfer of pigment epithelium-derived factor (PEDF) in animal models of RP; however, the underlying mechanism of the neuroprotective activity of PEDF remains elusive. In this study, we show that an apoptosis-inducing factor (AIF)-related pathway is an essential target of PEDF-mediated neuroprotection. PEDF rescued serum starvation-induced apoptosis, which is mediated by AIF but not by caspases, of R28 cells derived from the rat retina by preventing translocation of AIF into the nucleus. Nuclear translocation of AIF was also observed in the apoptotic photoreceptors of Royal College of Surgeons rats, a well-known animal model of RP that carries a mutation of the *Mertk* gene. Lentivirus-mediated retinal gene transfer of PEDF prevented the nuclear translocation of AIF *in vivo*, resulting in the inhibition of the apoptotic loss of their photoreceptors in association with up-regulated Bcl-2 expression, which mediates the mitochondrial release of AIF. These findings clearly demonstrate that AIF is an essential executioner of photoreceptor apoptosis in inherited retinal degeneration and provide a therapeutic rationale for PEDF-mediated neuroprotective gene therapy for individuals with RP. ***(Am J Pathol 2008, 173:1326–1338; DOI: 10.2353/ajpath.2008.080466)***

Retinitis pigmentosa (RP) is a group of retinal degenerative diseases resulting from rod and cone photoreceptor cell death, and a major cause of blindness in adults. RP is caused by mutation in various genes expressed in photoreceptors, the retinal pigment epithelium (RPE) and choriocapillaris of the eye[1,2]; on the other hand, photoreceptors undergo a common mode of cell death, apoptosis.[3,4] Despite extensive efforts to better understand and treat RP, the mechanisms underlying the photoreceptor apoptosis are still unclear and these diseases remain intractable.

Supported in part by the Japanese Ministry of Education, Culture, Sports, Science, and Technology (grants-in-aid 16390118, 17689047, and 19209012 to Y.I., Y.Y., and K.S.).

Accepted for publication August 7, 2008.

Competing Interest Statement: Y.Y. is a member of the Scientific Advisory Board of DNAVEC Corporation.

Supplemental material for this article can be found on *http://ajp.amjpathol.org.*

Address reprint requests to Katsuo Sueishi, M.D., Ph.D., Division of Pathophysiological and Experimental Pathology, Department of Pathology, Graduate School of Medical Sciences, Kyushu University, 3-1-1 Maidashi, Higashi-ku, Fukuoka, 812-8582, Japan. E-mail: sueishi@pathol1.med.kyushu-u.ac.jp.

Pigment epithelium-derived factor (PEDF) is a 50-kDa secreted glycoprotein that was isolated from the conditioned medium of human RPE,[5,6] and shows both neuroprotective and anti-angiogenic properties.[7,8] Vitreous samples from patients with RP contain significantly lower levels of PEDF than those from patients with other retinal conditions.[9] We previously demonstrated that a lentiviral vector based on the simian immunodeficiency virus from African green monkeys (SIVagm) showed sustained transgene expression in RPE of the rat retina,[10] and SIV-mediated retinal gene transfer of PEDF efficiently prevented photoreceptor apoptosis in Royal College of Surgeons (RCS) rats, an animal model of retinal degeneration caused by a *Mertk* mutation.[11] In addition, these protective effects of PEDF have also been observed in rds mice (M. Miyazaki et al, unpublished observations) and rd1 mice,[12] in which the deficits of photoreceptors are caused by different mutations, suggesting the possibility that PEDF might suppress a common pathway leading to the photoreceptor apoptosis. Several studies have demonstrated the direct protective effects on neuronal cells in culture,[13] but the precise mechanism by which PEDF acts on photoreceptors remains unknown.

The caspase family has emerged as a central regulator of apoptosis, especially in the developmental stages. However, recent evidence indicates that apoptosis can be induced by a caspase-independent pathway in several pathological states.[14] Apoptosis-inducing factor (AIF), a flavoprotein in the mitochondrial intermembrane space, has been identified as a caspase-independent apoptotic inducer,[15,16] and plays a prosurvival role through its redox activity under normal conditions.[17,18] AIF translocates to the nucleus during the apoptotic process, and causes peripheral chromatin condensation and large-scale fragmentation of DNA.[19,20] The translocation of AIF has been implicated in several types of neuronal demise, including photoreceptor apoptosis, and has been shown to contribute significantly to the apoptotic process.[21–23]

In the present study, we investigated the signaling pathways related to photoreceptor apoptosis that could be targets of the neuroprotective activity of PEDF *in vitro* and *in vivo*. We found that the nuclear translocation of AIF occurs in apoptotic photoreceptors in RCS rats, and that PEDF targets this process, resulting in the prevention of the apoptosis.

Materials and Methods

Reagents and SIV Vectors

The recombinant human (rhPEDF) was prepared as previously described.[24] His-tagged rhPEDF cloned into pCEP4 vector was isolated from medium conditioned by HEK293 cells. Polyclonal anti-hPEDF antibody was purchased from R&D Systems (Minneapolis, MN). The broad range caspase inhibitor Z-VAD-fmk was obtained from Peptide Institute (Osaka, Japan). Staurosporine was from Alomone Labs (Jerusalem, Israel). To produce third-generation recombinant SIVagm-based lentiviral vectors, HEK293T cells were transfected with the packaging vector, the gene transfer vectors encoding hPEDF (SIV-hPEDF) driven by the cytomegalovirus promoter, the Rev expression vector, and the envelope vector, pVSV-G (Clontech Laboratories, Inc., Mountain View, CA). The SIV vector lacking a transgene cassette (SIV-Empty) was used as the control vector. A U3 region in the 3′ and 5′ long terminal repeat of the SIVagm was deleted to induce self-inactivation. The virus titer was determined by a transduction of the HEK293T cells as expressed in transducing Us/ml, and these viruses were kept at −80°C until just before use.

Cell Culture and Viability Assay

R28 cells, an immortalized retinal precursor cell line derived from the rat retina at postnatal day 6, were the kind gift of Gail M. Seigel (The State University of New York, Buffalo, NY). R28 cells were cultured in Dulbecco's modified Eagle's medium-high glucose with 10% fetal bovine serum, 1× minimum essential medium, 1 × 10 mmol/L nonessential amino acids, 0.37% sodium bicarbonate, and 10 mg/ml gentamicin (Invitrogen, Carlsbad, CA). To induce cell death by serum starvation, R28 cells at 50% confluence were washed with phosphate-buffered saline (PBS) twice, and the culture medium was replaced with 100 μl of serum-free medium. After 6 hours for synchronization, rhPEDF or PBS was added to each well at the indicated concentration. After incubation for 48 hours, the cell viability was assessed by a Cell Counting Kit-8 (Dojindo Laboratories, Kumamoto, Japan). This assay is based on the cleavage of 2-(2-methoxy-4-nitrophenyl)-3-(4-nitrophenyl)-5-(2,4-disulfophenyl)-2H-tetrazolium, monosodium salt (WST-8) to formazan dye by the mitochondrial dehydrogenase enzyme. After incubation with WST-8 for 2 hours at 37°C, the absorbance was measured at 450 nm using a microplate leader. The absorbance was directly proportional to the number of living cells (data not shown).

Animals

Adult RCS rats and age-matched Wistar rats were maintained humanely with proper institutional approval, and in accordance with the statement of the Association for Research in Vision and Ophthalmology. All animal experiments were performed under approved protocols and in accordance with the recommendations for the proper care and use of laboratory animals by the Committee for Animals, Recombinant DNA, and Infectious Pathogens Experiments at Kyushu University and according to The Law (no.105) and Notification (no.6) of the Japanese Government.

Gene Transfer Procedures

The subretinal injection of each solution was performed as previously described.[11,25] Briefly, 3-week-old RCS rats were anesthetized by inhalation ether. A 30-gauge needle was inserted into the subretinal space of the peripheral retina in the nasal hemisphere via an external

transscleral transchoroidal approach. The vector solution (SIV-hPEDF or SIV-Empty; 2.5×10^7 transducing U/ml $\times$ 10 μl) was injected, and excess solution from the injection site was washed out using PBS. Approximately 3 μl of solution remained in the subretinal space (data not shown). The appearance of a dome-shaped retinal detachment confirmed the subretinal delivery. Eyes that sustained prominent surgical trauma, such as retinal or subretinal hemorrhage or bacterial infection, were excluded from this examination.

Histological Examination

At 2 weeks after gene transfer, the eyes of animals were enucleated and frozen in liquid nitrogen, and 5-μm-thick cryosections were prepared along the horizontal meridian. The sections were stained with hematoxylin and eosin, and the number of photoreceptors was counted per 100 μm at 10 points as previously described (A1 to A5: from the ora serrata to the optic nerve of the nasal hemisphere; A6 to A10: from the optic nerve to the ora serrata of the temporal hemisphere).[11]

Immunocytochemistry

R28 cells were fixed in 4% paraformaldehyde for 15 minutes, and then rinsed with PBS at room temperature. The cells were blocked with 3% nonfat dried milk and labeled with rabbit anti-AIF antibody (1:100; Cell Signaling Technology, Danvers, MA) at 4°C for 24 hours. After biotinylated goat anti-rabbit IgG (H+L) (1:200; Vector Laboratories, Burlingame, CA) was used as a secondary antibody, the cells were incubated with r-phycoerythrin (PE)-conjugated or fluorescein isothiocyanate-conjugated streptavidin (1:100; BD Biosciences, San Diego, CA). After labeling, propidium iodide or 4,6-diamidino-2-phenylindole (DAPI) was used to counterstain the nuclei. Immunofluorescence images were acquired using an Olympus BX51 microscope with a fluorescent attachment (Tokyo, Japan). For negative controls, the primary antibody was omitted.

Immunohistochemistry

Rats were sacrificed under deep anesthesia. The eyes were removed and frozen in OCT compound (Sakura Finetechnical Co., Tokyo, Japan). Five-μm-thick sections were cut, air-dried, and fixed in cold acetone for 10 minutes. For a primary antibody, rabbit anti-AIF antibody (1:100; Cell Signaling Technology) was used. The specimens were imaged with a laser-scanning confocal microscope (LSM-GB200, Olympus).

Terminal dUTP Nick-End Labeling (TUNEL) Staining

The TUNEL procedure and quantification of TUNEL-positive cells were performed using an ApopTag fluorescein direct *in situ* apoptosis detection kit (Chemicon International, Temecula, CA) for R28 cultures or an Apoptosis Detection TACS TdT Kit (R&D Systems) for retinal sections according to the instructions of the manufacturer. The number of TUNEL-positive cells was counted in a masked manner.

Flow Cytometry Analysis

The population of early apoptotic cells was analyzed using an Annexin V-PE Apoptosis Detection Kit I (BD Biosciences). After serum starvation, R28 cells were harvested, washed twice with ice-cold PBS, and resuspended in 100 μl of calcium-binding buffer (10 mmol/L Hepes/NaOH, pH 7.4, 140 mmol/L NaCl, 2.5 mmol/L $CaCl_2$). The cells were double-labeled with Annexin V-PE (1:20) for the assessment of phosphatidylserine exposure and 7-amino-actinomycin D (7-AAD) (1:20) for cell viability analysis. After 15 minutes of incubation in the dark, the cells were diluted with 400 μl of binding buffer. Samples were analyzed in a FACScan flow cytometer (Becton Dickinson, San Jose, CA) using the program CellQuest (Becton Dickinson) for subsequent data treatment. A total of 5000 events per sample were acquired, and Annexin V-PE-positive and 7-AAD-negative events were defined as early apoptotic cells.

Western Blotting

Eighty μg of protein was separated on sodium dodecyl sulfate-polyacrylamide gel electrophoresis and transferred to the membrane. After blocking with 3% nonfat dried milk, the membrane was reacted with anti-AIF antibody (Calbiochem, San Diego, CA), anti-cleaved caspase-3, anti-Bcl-2, or anti-Bax antibody (Cell Signaling Technology). The immunoreactivity was visualized using the ECL Plus detection reagents (Amersham Biosciences, Buckinghamshire, UK).

Enzyme-Linked Immunosorbent Assay (ELISA)

The protein contents in rat eyes were determined using an ELISA kit for human PEDF (not available for rat PEDF; Chemicon International). For ocular tissue preparation, conjunctival and muscular tissues were removed from enucleated eyes. The eyes were washed with PBS, minced with scissors in 500 μl of 1$\times$ lysis buffer with a protease inhibitor cocktail, and centrifuged at 15,000 rpm for 5 minutes at 4°C. The supernatants were subjected to ELISA according to the manufacturer's instructions.

RNAi

AIF siRNA was synthesized with the sequence 5′-GCAACCUAGUAUACUUCUUTT-3′. The scrambled counterpart, control siRNA, had the sequence 5′-GCAUCGAAUAUUCUAC-CUUTT-3′. The sequence of Bcl-2 siRNA was 5′-AUGGAUGUACUUCAUCACGAUCUCC-3′, and the negative control kit Medium GC was used as a control (Invitrogen). Transfection of 40 nmol/L siRNA was performed using Lipofectamine 2000 reagent (Invitrogen) according to the manufacturer's instructions.

RNA Extraction and Quantitative Real-Time Polymerase Chain Reaction (PCR)

The procedures for RNA extraction were described previously.[26] The total RNA was extracted from the R28 cells or the neural retina by Isogen (Nippon Gene Co., Osaka, Japan) followed by treatment with RNase-free DNase I. The RNA was then reverse-transcribed and amplified with the TaqMan EZ RT-PCR kit and a sequence detection system, model 7000 (Applied Biosystems, Foster City, CA). The PCR primers used in this study were as follows: rat Bcl-2 forward, 5′-CTGGGATGCCTTTGTGGAA-3′; rat Bcl-2 reverse, 5′-CAGAGACAGCCAGGAGAAATCA-3′; rat Bcl-2 hybridization probe, 5′-FAM-ATGGCCCCAGCATGCGACCTC-TAMRA-3′; rat Bax forward, 5′-CGTGGTTGCCCTCT TCTACTTT-3′, rat Bax reverse, 5′-TGATCAGCTCGGGCACTTTA-3′; rat Bax hybridization probe, 5′-FAM-CTAGCAAACTGGTGCTCAAGGCCCTG-TAMRA-3′; rat β-actin forward, 5′-CCCTGGCTCCTAGCACCAT-3′; rat β-actin reverse, 5′-CCTGCTTGC-TGATCCACATCT-3′; and rat β-actin hybridization probe, 5′-FAM-CCTGGCCTCACTGTCCACCTTCCA-TAMRA-3′. The expression level of the target gene was normalized by the β-actin level in each sample.

MitoTracker Staining

R28 cells were incubated with a 50 nmol/L solution of MitoTracker Orange CMTMRos (Invitrogen), a derivative of tetramethylrosamine, for 15 minutes at 37°C. The MitoTracker probe passively diffuses across the plasma membrane and accumulates in active mitochondria, driven by the mitochondrial inner transmembrane potential.[27,28] After incubation, the cells were fixed in 4% paraformaldehyde for 15 minutes, labeled with DAPI, and observed under a fluorescence microscope.

Statistical Analyses

All values were expressed as the mean ± SD. The data were analyzed by the two-tailed unpaired Student's *t*-test. Numbers per group were as indicated. A *P* value less than 0.05 was considered statistically significant.

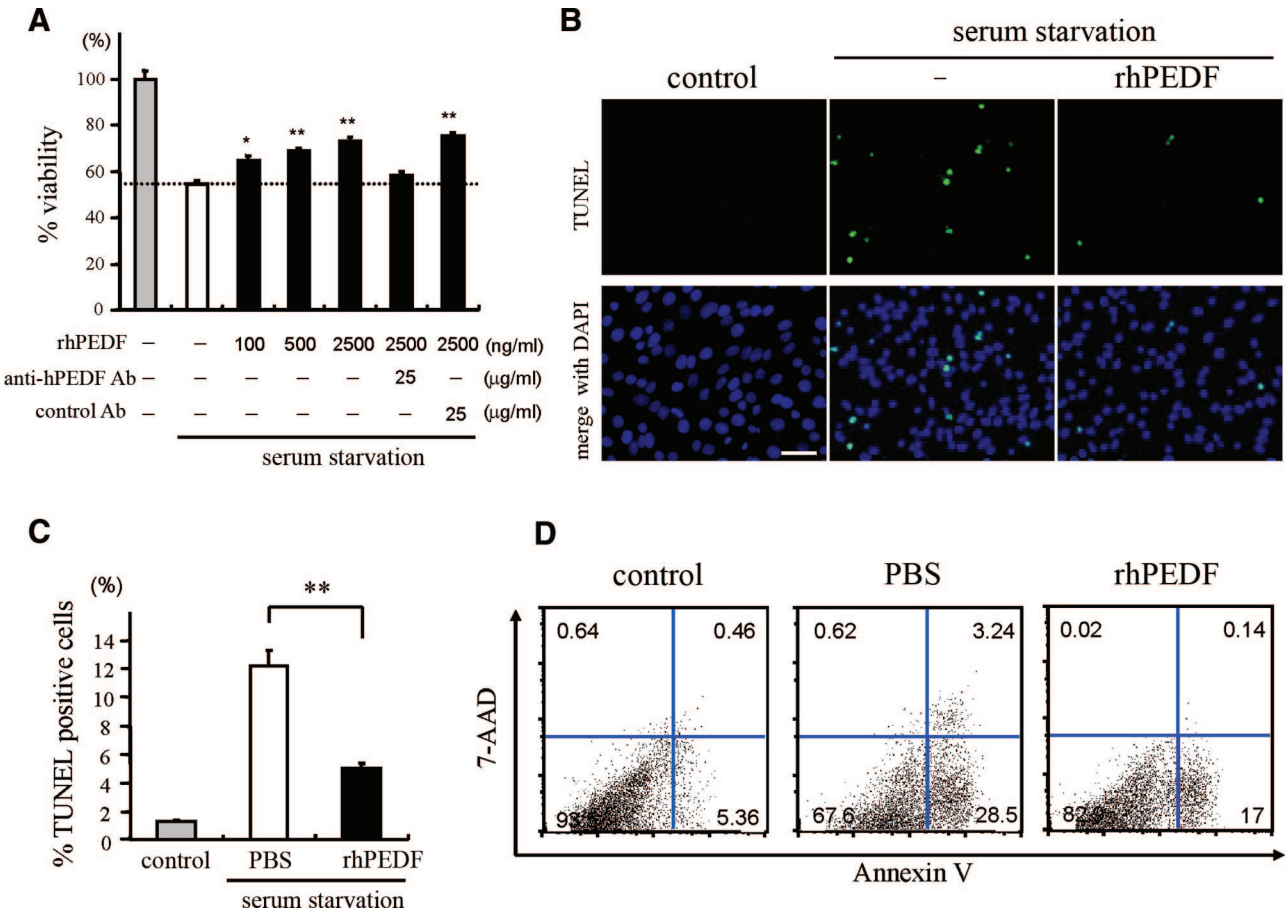

Figure 1. PEDF rescues apoptosis induced by serum starvation in R28 cells. **A:** The effect of PEDF on cell viability. R28 cells were serum-deprived and treated with PBS or rhPEDF at the indicated doses. After 48 hours of culturing, the cell viability was assessed by WST-8 colorimetric assay ($n = 4$ each). The effect of PEDF was reversed by anti-PEDF antibody but not by nonimmune control antibody. $^{*}P < 0.05$ and $^{**}P < 0.01$ versus PBS-treated samples. **B** and **C:** TUNEL staining (**B**) and quantitative analysis of the TUNEL-positive apoptotic nuclei (**C**) in serum-starved R28 cells treated with PBS (white bar) or rhPEDF (black bar) ($n = 5$ each). The cells growing in serum-containing medium were used as controls (gray bar). $^{**}P < 0.01$. **D:** Flow cytometry analysis of the apoptotic population after 48 hours of serum starvation. Cells were stained with Annexin V and 7-AAD. The percentages of Annexin V-positive and 7-AAD-negative early apoptotic cells were 28.3 ± 0.15% in PBS-treated cells and 17.7 ± 0.34% in rhPEDF-treated cells ($n = 4$ each). Scale bar = 50 μm.

Results

Effects of PEDF on Serum Starvation-Induced Apoptosis in R28 Cultures

The R28 cell line was derived from the rat retina on postnatal day 6 and has been shown to express neuronal genes.[29] To investigate whether PEDF can act as a survival factor for R28, we first cultured R28 cells under a serum-starved condition with or without rhPEDF, and assessed the cell viability by WST-8 colorimetric assay after 48 hours of culturing. Treatment with rhPEDF dose dependently rescued serum starvation-induced cell death and 41.1% of the reduction of cell viability was rescued by 2500 ng/ml rhPEDF ($P < 0.01$ versus PBS-treated R28 cells; Figure 1A). The effect of rhPEDF was completely reversed by treatment with polyclonal anti-hPEDF antibodies (25 μg/ml) (Figure 1A). The vitreous of the human eye contains 0.5 to 5 μg/ml of hPEDF protein,[30,31] and thus the concentrations of rhPEDF used in this experiment were in a physiological range. TUNEL staining revealed that ~10% of cells were TUNEL-positive apoptotic cells after 48 hours of serum starvation (12.2 ± 1.13%); by contrast, treatment with rhPEDF significantly reduced the frequency of TUNEL-positive cells (5.1 ± 0.26%, $P = 0.0002$; Figure 1, B and C). Less than 2% of cells were TUNEL-positive under control conditions. The apoptotic population was also assessed by fluorescence-activated cell sorter analysis of Annexin V/7-AAD staining. The percentages of early apoptotic cells that were defined as Annexin V-PE-positive and 7-AAD-negative were significantly lower in rhPEDF-treated cells (17.7 ± 0.34%) than PBS-treated cells (28.3 ± 0.15%, $P < 0.0001$; Figure 1D). Together, these results indicate that PEDF inhibits the apoptosis induced by serum starvation in R28 cells. RT-PCR analysis revealed that R28 cells strongly expressed the PEDF receptor, which was identified in a recent study (data not shown).[32]

A Minor Role of Caspases in Serum Starvation-Induced Apoptosis in R28 Cells

To elucidate the molecular events during serum starvation-induced apoptosis, we next examined the involvement of caspases. First, we performed Western blot analysis of caspase-3, a key effector of caspase-dependent apoptosis. As shown in Figure 2A, a 17-kDa active form of caspase-3 was detected at 48 hours after serum starvation. To elucidate the exact contribution of caspases, we next cultured R28 cells under a serum-starved condition, in the presence or absence of Z-VAD-fmk, a broad range caspase inhibitor. Treatment with Z-VAD-fmk (10 μmol/L) completely abrogated the cleavage of caspase-3 induced by serum starvation (Figure 2A), but this treatment showed no beneficial effect on the cell viability (Figure 2B). The doses higher than 10 μmol/L were cytotoxic, reducing the levels of cell viability (data not shown). These results suggest that caspases are not the major executioners of serum starvation-induced apoptosis. By contrast, the cell death induced by staurosporine, a potent activator of caspases, was significantly rescued by treatment with Z-VAD-fmk (10 μmol/L) (Figure 2C). Interestingly, rhPEDF had no significant effect on either the cell viability or the cleavage of caspase-3 after staurosporine treatment (Figure 2, C and D), suggesting that PEDF might be involved in a caspase-independent pathway.

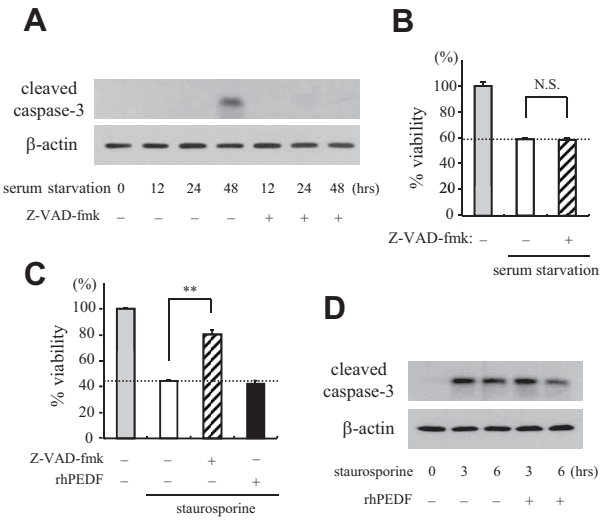

Figure 2. The role of caspases in serum starvation-induced apoptosis. **A:** Analysis of activation of caspase-3 after serum starvation. Total proteins were purified from R28 cells that were serum-deprived for the indicated period of time with or without Z-VAD-fmk (10 μmol/L), and subjected to Western blotting with an antibody against cleaved caspase-3 (**top**). Lane-loading differences were normalized by the level of β-actin (**bottom**). The panels show the representative results from three independent experiments. **B:** The inhibition of caspases did not rescue serum starvation-induced cell death. R28 cells were cultured under a serum-starved condition for 48 hours in the presence or absence of Z-VAD-fmk (10 μmol/L) before assessing the cell viability ($n = 4$ each). **C:** Staurosporine-induced cell death was rescued by Z-VAD-fmk, but not by PEDF. R28 cells were cultured with 100 nmol/L staurosporine for 24 hours in the presence of PBS, Z-VAD-fmk (10 μmol/L), or rhPEDF (2500 ng/ml), and the cell viability was assessed ($n = 4$ each). $^{**}P < 0.01$. **D:** The effect of PEDF on caspase-3 activation induced by staurosporine. Total proteins were purified from R28 cells that were treated with staurosporine for the indicated period of time with or without rhPEDF (2500 ng/ml). Western blotting showed that the expression level of cleaved caspase-3 was unchanged by rhPEDF.

Role of AIF in Serum Starvation-Induced Apoptosis and Effects of PEDF on AIF Relocalization

AIF is a mitochondrial flavoprotein that is released in response to death stimuli and induces apoptosis independently of caspases after nuclear translocation.[20] To examine whether serum starvation-induced apoptosis involved AIF, we next analyzed the changes in subcellular localization of AIF by immunocytochemistry. In control R28 cells, AIF was excluded from the nucleus and displayed a punctate staining pattern in the cytoplasm. By contrast, after 48 hours of serum starvation, 17.5 ± 4.6% of the cells showed diffuse staining and nuclear translocation of AIF (Figure 3, A and B). No positive staining was found by nonimmune IgG (data not shown). Double-labeling with TUNEL showed that ~75% of AIF-positive nuclei were also TUNEL-positive (Figure 3, C and D). Furthermore, treatment with rhPEDF dramatically pre-

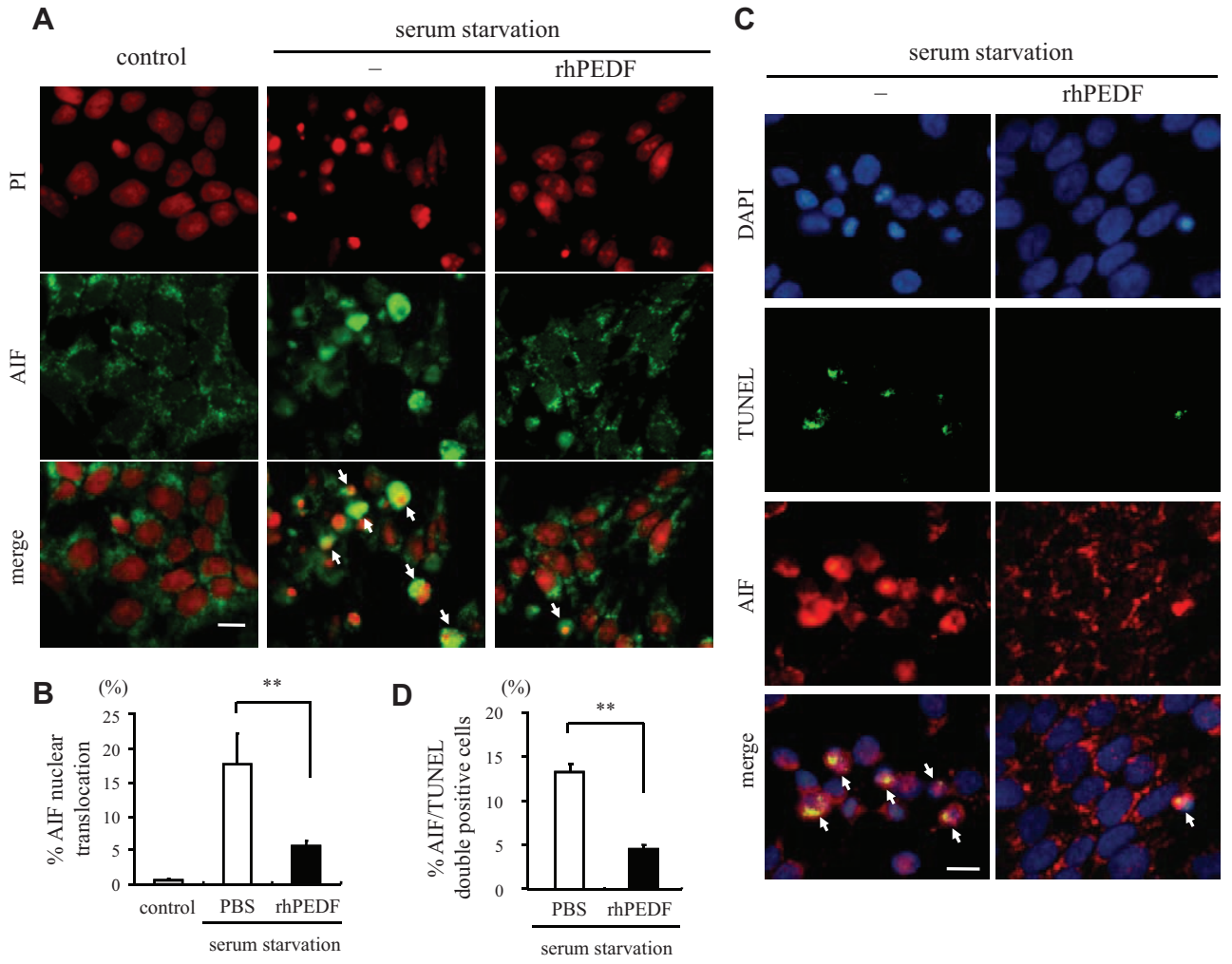

Figure 3. AIF nuclear translocation during serum starvation-induced apoptosis and effect of PEDF on the AIF release. **A:** Immunocytochemistry of AIF after serum starvation. After 48 hours of culturing in serum-starved medium with or without rhPEDF (2500 ng/ml), the R28 cells were stained with an anti-AIF antibody. The cells growing in serum-containing medium were used as controls. The nuclei were counterstained with propidium iodide. **Arrows** indicate the translocation of AIF into the nucleus. **B:** Quantification of cells showing nuclear translocation of AIF in control (gray bar) or serum-starved R28 cells treated with PBS (white bar) or rhPEDF (black bar) ($n = 5$ each). $^{**}P < 0.01$. **C** and **D:** Double-staining for AIF and TUNEL (**C**) and the quantification of AIF/TUNEL double-positive apoptotic nuclei (**D**) after serum starvation ($n = 5$ each). The nuclei were counterstained with DAPI. **Arrows** indicate the co-localization of AIF and TUNEL. $^{**}P < 0.01$. Scale bars = 10 μm.

vented the nuclear translocation of AIF after serum starvation (5.6 ± 0.74%, $P = 0.0066$ versus PBS-treated samples; Figure 3, A and B) and reduced the number of AIF/TUNEL double-positive cells ($P < 0.0001$ versus PBS-treated samples; Figure 3, C and D).

To further address the role of AIF in serum starvation-induced apoptosis, we used RNAi to knockdown AIF in R28 cells. siRNA for AIF, but not randomized control siRNA, showed efficient down-regulation of AIF (Figure 4A). When AIF was down-regulated, 33.1% of the reduction of cell viability after 48 hours of serum starvation was rescued ($P = 0.0002$ versus R28 cells treated with randomized control siRNA; Figure 4B). TUNEL-positive apoptotic cells were also significantly reduced in cells treated with siRNA for AIF (6.6 ± 1.30%) compared to cells treated with randomized control siRNA (13.6 ± 0.76%, $P = 0.0031$; Figure 4, C and D). In addition, treatment with rhPEDF showed no significant effect on the frequency of TUNEL-positive cells in samples with AIF down-regulation (5.39 ± 1.11%, $P = 0.53$; Figure 4, C and D). Together, these results indicate that AIF is an important executioner of serum starvation-induced apoptosis, and that PEDF inhibits the apoptosis by preventing the AIF nuclear translocation.

PEDF Prevents AIF Translocation and Photoreceptor Apoptosis in RCS Rats

To further examine the role of PEDF *in vivo*, we next assessed the effect of exogenously overexpressed PEDF on the degeneration of photoreceptors in RCS rats. P21 RCS rats received subretinal injection of SIV-hPEDF or SIV-Empty in the nasal peripheral retinas. First, we confirmed the efficient gene transfer and expression of hPEDF after subretinal injection of SIV-hPEDF by ELISA (Figure 5A). The gene transfer of hPEDF was observed in the RPE in the vector-injected area as previously de-

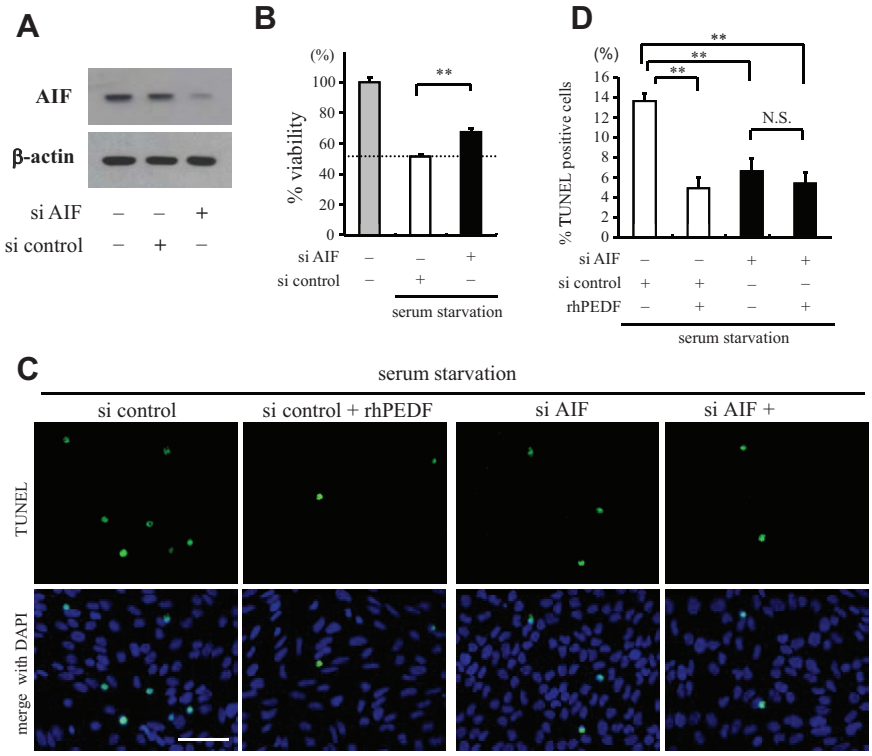

Figure 4. Knockdown of AIF mRNA rescues R28 apoptosis after serum starvation. **A:** Western blot analysis for AIF in RNAi experiments. Total proteins were purified from R28 cells 48 hours after transfection of siRNA for AIF or randomized control siRNA (**top**). Lane-loading differences were normalized by the level of β-actin (**bottom**). The panels show the representative results from three independent experiments. **B:** The siRNA targeting AIF or randomized control siRNA were transfected to R28 cells before the serum starvation assay. The cell viability was assessed after culturing in serum-free medium for 48 hours ($n = 4$ each). $^{**}P < 0.01$. **C** and **D:** TUNEL staining (**C**) and quantitative analysis of the TUNEL-positive cells (**D**) in serum-starved R28 cells treated with randomized control siRNA (white bar) or siRNA targeting AIF (black bar) and the effect of rhPEDF (2500 ng/ml) on these cells ($n = 5$ each). $^{**}P < 0.01$. Scale bar = 50 μm.

scribed (data not shown).[11] At 2 weeks after the gene transfer, the number of photoreceptors was counted per 100 μm at 10 points along the horizontal meridian of the eyes. As shown in Figure 5, B and C, the retinas treated with SIV-hPEDF demonstrated significant rescue of photoreceptors in the nasal hemisphere, compared to retinas that were untreated or treated with SIV-Empty ($P < 0.05$). The region nearest the vector-injected site (A1 to A3) showed the greatest prevention of photoreceptor cell death, and thus we assessed the retinas in areas A1 to A3 in the following experiments. The percentage of TUNEL-positive photoreceptor nuclei in the outer nuclear layer was ~3.5% in the untreated or SIV-Empty-treated retinas, whereas it was significantly decreased in the SIV-hPEDF-treated retinas (0.8 ± 0.07%, $P < 0.01$; Figure 5, D and E). Throughout the study period, neither severe inflammation nor morphological change of RPE was seen in any of the retinas. Next, we conducted double-staining of AIF and TUNEL in these retinas. Immunohistochemistry of control normal retinas showed a positive staining for AIF in the inner segment (IS) of photoreceptors, which were a mitochondrion-rich portion of cells. In RCS rats that were untreated or treated with SIV-Empty, the AIF distribution in the IS was disrupted and AIF translocation was observed in most of the TUNEL-positive nuclei (percentage of AIF/TUNEL double-positive nuclei: 3.4 ± 0.38% and 3.2 ± 0.56%, respectively). By contrast, treatment with SIV-hPEDF relatively preserved the distribution and significantly reduced the AIF translocation into the nuclei (0.6 ± 0.05%, $P < 0.01$; Figure 6). At 4 weeks after the gene transfer, the SIV-hPEDF-treated retinas also showed the reduction of AIF nuclear translocation and had more than twice the number of photoreceptor nuclei compared to untreated or SIV-Empty-treated retinas. However, the number of photoreceptors was reduced by half in comparison with that at 2 weeks after vector injection, indicating that the retinal degeneration was delayed but not completely prevented by the gene transfer of hPEDF (see Supplementary Figure S1 at *http://ajp.amjpathol.org*). These findings were consistent with the *in vitro* data, and indicate that PEDF prevents the translocation of AIF, resulting in a substantial protection of photoreceptors during retinal degeneration.

PEDF Prevents AIF Translocation through Bcl-2 Up-Regulation

During apoptosis, AIF is released after the loss of mitochondrial membrane potential,[33] and this release is inhibited by overexpression of Bcl-2, which preserves the mitochondrial integrity.[15,34] Based on the findings that PEDF prevents AIF translocation both *in vitro* and *in vivo*, we finally asked whether PEDF affects the mitochondrial function and the expression of pro- and anti-apoptotic Bcl-2 family members. To examine the changes in mitochondrial membrane potential during serum starvation-induced apoptosis, R28 cells were co-cultured with a mitochondrial potential-sensitive dye, MitoTracker CMTMRos. In control R28 cells, the mitochondria exhibited a punctate staining pattern with MitoTracker CMTMRos. After 48 hours of serum starvation, 16.7 ± 2.60% of the cells showed the loss of MitoTracker staining, indicating the mitochondrial depolarization. This effect was significantly reversed by rhPEDF treatment (4.9 ± 1.29%, $P = 0.0068$; Figure 7A). Next, we assessed the transcriptional

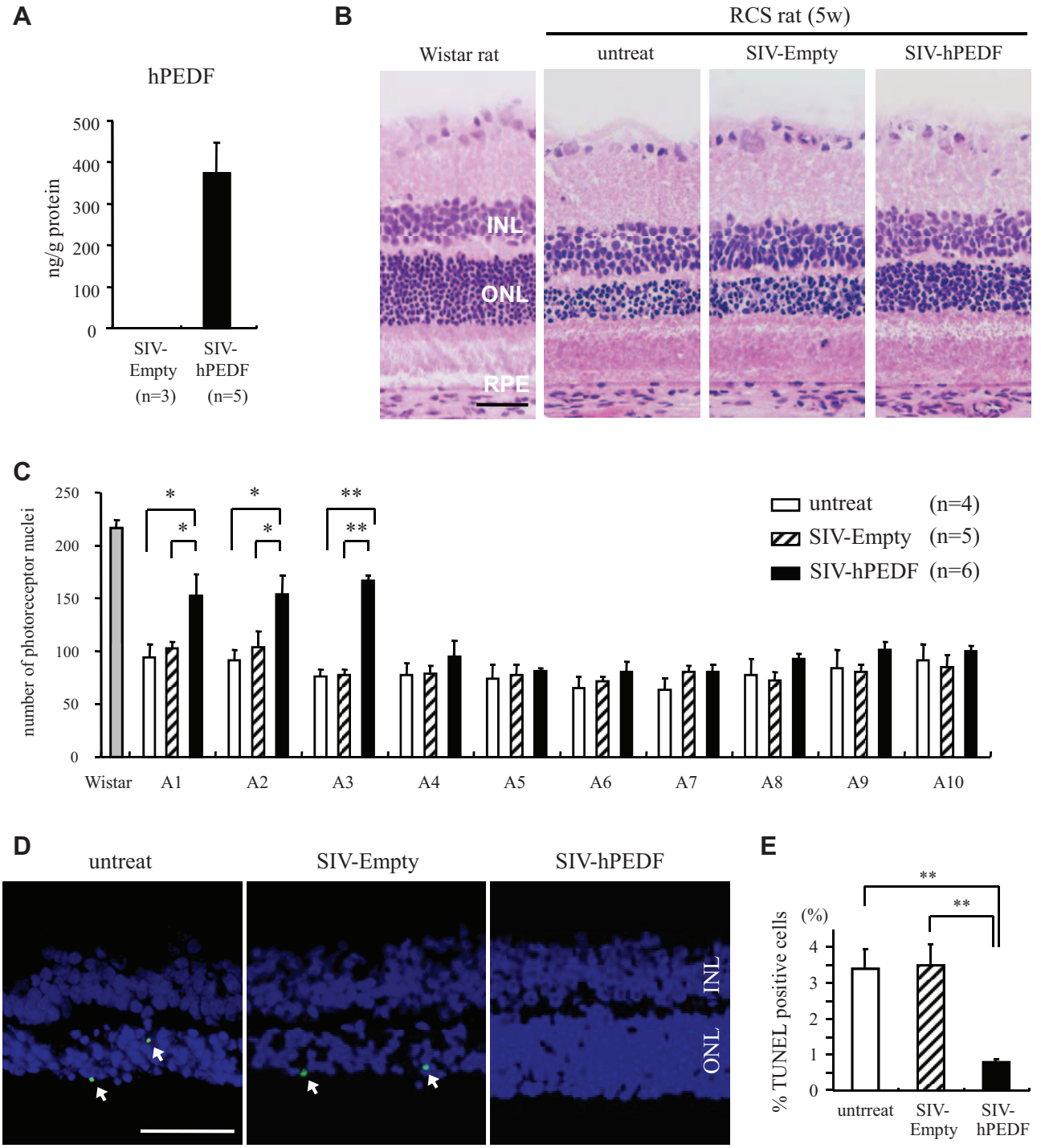

Figure 5. SIV vector-mediated retinal gene transfer of PEDF prevents photoreceptor apoptosis in RCS rats. **A:** ELISA to detect hPEDF protein at 2 weeks after subretinal injection of SIV-hPEDF into the nasal peripheral retinas of RCS rats (n = 3 to 5). **B:** Histological findings of the nasal retina of untreated RCS rats, and RCS rats treated with SIV-Empty or SIV-hPEDF at 2 weeks after injection. The retinas of Wistar rats were used as a control. INL, inner nuclear layer; ONL, outer nuclear layer. RPE indicates retinal pigment epithelium, which tie at the outer layer of retina. **C:** Quantitative analysis of photoreceptor nuclei in RCS rats. The number of photoreceptors per 100 μm was counted at 10 points along the horizontal meridian of the eye (A1 to A10) (n = 4 to 6). The region A1 to A5 corresponds to the nasal hemisphere of the eye. $^{*}P < 0.05$ and $^{**}P < 0.01$. **D** and **E:** TUNEL staining (**D**) and quantitative analysis of the TUNEL-positive photoreceptor nuclei (**E**) in RCS rats at 2 weeks after vector injection (n = 4 to 6). $^{*}P < 0.05$ and $^{**}P < 0.01$. Scale bars = 50 μm. The **arrows** indicate the TUNEL-positive photoreceptor nuclei.

changes in Bax and Bcl-2 expression by quantitative real-time PCR. In R28 cells, treatment with rhPEDF resulted in a 1.7-fold increase of Bcl-2 expression at 6 hours after stimulation (P = 0.0206 versus PBS-treated samples; Figure 7B). The level of Bax expression was almost unchanged. In RCS rats, Bcl-2 expression increased twofold in the neural retina treated with SIV-hPEDF, compared to that in untreated or SIV-Empty-treated rats ($P < 0.03$; Figure 7C). Western blot analysis confirmed that the protein expression of Bcl-2 was up-

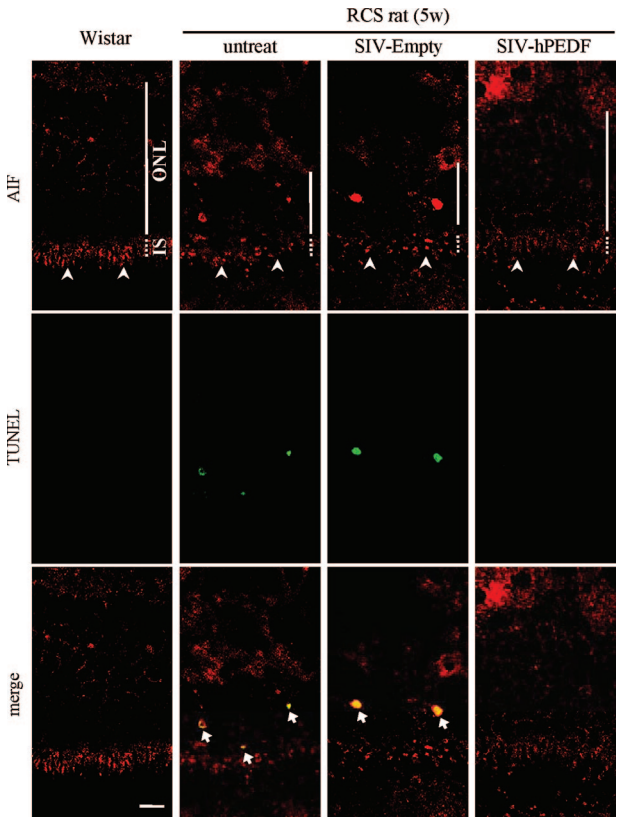

Figure 6. PEDF inhibits AIF translocation in photoreceptors of RCS rats. Confocal microscopy of the nasal retina double-stained with AIF and TUNEL at 2 weeks after vector injection. The **arrowheads** indicate the distribution of AIF in the IS of photoreceptors and the **arrows** indicate the co-localization of AIF and TUNEL. Scale bar = 10 μm.

regulated in R28 cells and the eyes of RCS rats by treatment with PEDF (Figure 7, D and E). To further examine the role of Bcl-2 in the PEDF-mediated inhibition of AIF release, we performed knockdown experiments in R28 cells. siRNA for Bcl-2, but not control siRNA, showed efficient down-regulation of Bcl-2 (Figure 7F), and attenuated the effect of PEDF on AIF nuclear translocation after serum starvation (Figure 7, G and H). Together, these data indicate that PEDF prevents the loss of mitochondrial membrane potential and inhibits AIF nuclear translocation by inducing Bcl-2 expression.

Discussion

Molecular genetic analyses of inherited retinal degeneration have identified 40 different genetic mutations accounting for only a minority of RP patients [Retinal Information Network (RetNet) at *http://www.sph.uth.tmc.edu/Retnet/*]. Despite advances in our understanding of the genetic heterogeneity of RP, the mechanism by which photoreceptors execute apoptosis is primarily unknown and is a matter of continuing debate. In the present study, we investigated the signaling pathways that are directly related to the neuroprotective activity of PEDF in retinal degeneration. The key observations made in this study are as follows: i) PEDF efficiently rescued apoptosis induced by serum starvation but not by staurosporine in R28 cells derived from rat retina; ii) AIF but not caspases was a key effector of the serum starvation-induced apoptosis, and PEDF prevented AIF from translocating into the nucleus after serum starvation; iii) Nuclear translocation of AIF was also observed in apoptotic photoreceptors of RCS rats, and was significantly inhibited by retinal gene transfer of PEDF *in vivo*, resulting in a substantial delay in retinal degeneration; and iv) PEDF prevented the AIF release through up-regulation of Bcl-2. These findings clearly demonstrated that the AIF-mediated pathway is an essential target of PEDF during the photoreceptor apoptosis in retinal degeneration.

There has been an increasing body of evidence suggesting that caspases are not essential for photoreceptor apoptosis in animal models of retinal degeneration. In the mature brain and retina, it has been demonstrated that caspase-dependent apoptosis is down-regulated because of a differentiation-associated reduction in apoptosis proteases-activating factor-1 expression and increased efficacy of inhibitors of apoptosis proteins.[35–37] Segura and colleagues[38] recently reported that the long form of the Fas apoptotic inhibitory molecule is predominantly expressed in neurons and prevents the activation of caspase-8 induced by Fas. During photoreceptor apoptosis in rd1 mice or light-induced retinal injury, caspases were not activated and the apoptosis was not prevented by a broad-range caspase inhibitor or gene ablation of caspase-3.[36,39–41] We also observed that treatment with Z-VAD-fmk showed no significant protective effect on retinal degeneration in RCS rats (see Supplementary Figure S2 at *http://ajp.amjpathol.org*). These findings strongly suggest the presence of a caspase-independent mechanism in retinal degeneration; however, it has remained unclear which pathways are actually involved in the apoptotic process. In the present study, we demonstrated for the first time that nuclear translocation of AIF was observed in apoptotic photoreceptors of RCS rats, which carry a mutation of the receptor tyrosine kinase *Mertk* (Figure 6). Recently, Sanges and colleagues[41] reported that AIF also significantly contributes to photoreceptor apoptosis in rd1 mice, which is caused by a mutation in the gene for the β-subunit of rod photoreceptor cGMP phosphodiesterase *PDE6B*, and thus it may be possible that nuclear translocation of AIF is a common pathway in inherited retinal degeneration irrespective of the genetic status. Further studies will be needed to clarify the role of AIF in other models of retinal degeneration with different mutations.

In culture, we showed that R28 cell apoptosis induced by serum starvation could occur independently of caspase activation. The cell death was not rescued by the broad range caspase inhibitor Z-VAD-fmk (Figure 2B). It is unlikely that the caspase blockade was insufficient under this condition, because the activation of caspase-3 after serum starvation was completely abrogated and the cell death induced by staurosporine was significantly rescued by treatment with Z-VAD-fmk (Figure 2, A and C). By contrast, many of the apoptotic cells showed nuclear translocation of AIF, and siRNA-mediated knockdown of AIF resulted in a significant rescue of the apoptosis (Figures 3 and 4). Consistent with our

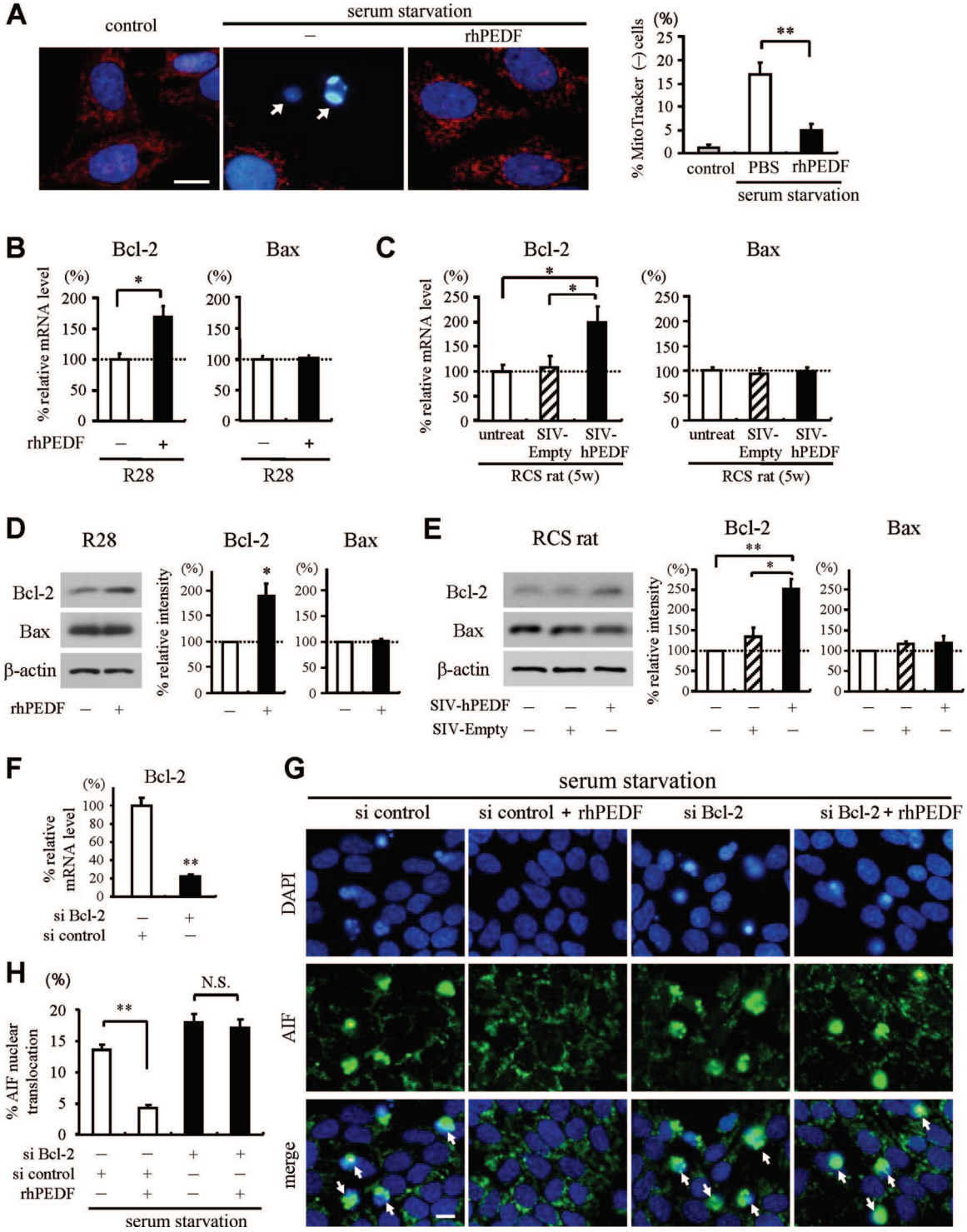

Figure 7. The effect of PEDF on mitochondrial function and expression of Bcl-2 family members. **A:** Mitochondrial function was assessed by a mitochondrial membrane potential-sensitive dye, MitoTracker CMTMRos. MitoTracker intake (MitoTracker in red, DAPI in blue) was lost in pyknotic R28 cells after 48 hours of serum starvation (**arrows**), but reversed in cells treated with rhPEDF (2500 ng/ml). The **right** panel shows the quantified results. $^{**}P < 0.01$. **B** and **C:** Quantitative real-time PCR analysis for Bcl-2 and Bax in PEDF-treated R28 cells (**B**) and neural retinas of RCS rats (**C**). **B:** R28 cells treated with rhPEDF or PBS were harvested and subjected to quantitative real-time PCR analysis at 6 hours after stimulation ($n = 4$ each). $^{*}P < 0.03$. **C:** At 2 weeks after vector injection, the neural retinas of untreated RCS rats or RCS rats treated with SIV-Empty or SIV-hPEDF were subjected to quantitative real-time PCR analysis ($n = 5$ to 6). $^{**}P < 0.03$. **D** and **E:** Western blot analysis for Bcl-2 and Bax in R28 cells after 24 hours of rhPEDF treatment (**D**) and in the eyes of RCS rats at 2 weeks after vector injection (**E**). Lane-loading differences were normalized by the level of β-actin. The bar graphs indicate the relative level of Bcl-2 or Bax to β-actin by densitometric analysis, reflecting the results from three independent experiments. $^{*}P < 0.05$ and $^{**}P < 0.01$. **F:** Quantitative real-time PCR analysis for Bcl-2 in R28 cells transfected with control siRNA or siRNA targeting Bcl-2 ($n = 3$ each). $^{**}P < 0.01$. **G** and **H:** Immunocytochemistry of AIF (**G**) and quantitative analysis of cells showing AIF nuclear translocation (**H**). Down-regulation of Bcl-2 in R28 cells attenuated the effect of PEDF on AIF nuclear translocation after serum starvation. Scale bars = 10 μm. The **arrows** indicate the cells showing AIF nuclear translocation.

findings, Klein and colleagues[17] reported that the primary granule cells derived from *Harlequin* (*Hq*) mutant mice, in which the AIF expression is reduced to 20% by proviral insertion, are resistant to cell death induced by serum starvation but not to cell death induced by staurosporine. These data suggest that AIF plays an essential role in serum starvation-induced apoptosis. Nuclear translocation of AIF is induced by several death stimuli after mitochondrial outer membrane permeability.[33,42,43] Although the mechanism leading to AIF release is still elusive, recent studies have demonstrated that AIF must be cleaved to be released from mitochondria, unlike other toxic proteins in the mitochondrial intermembrane space.[43,44] It has been shown that proteases such as calpains or cathepsins are involved in AIF cleavage and subsequent neuronal cell death,[45–47] and these proteases might play a role in triggering AIF release after serum starvation.

More interestingly, our data showed that PEDF dramatically prevents the translocation of AIF, resulting in significant inhibition of apoptosis in RCS rats and serum-starved R28 cells. The intracellular signaling pathways by which PEDF acts on neuronal cells have been explored mainly in culture, and the participation of NF-κB and cAMP-responsive element binding protein pathways has been demonstrated[13,48]; however, very little information is available regarding the downstream target molecules. An important advance of the current study, therefore, was that AIF was identified as an essential target molecule during PEDF-mediated neuroprotection both *in vitro* and *in vivo*. Moreover, we showed that the effect of PEDF on the AIF nuclear translocation is mediated by up-regulation of Bcl-2 expression (Figure 7), which directly regulates the mitochondrial membrane permeability and the AIF release.[15,49] However, it is less clear how PEDF up-regulates Bcl-2 gene expression. Notari and colleagues[32] recently determined that adipose triglyceride lipase (ATGL) is a receptor of PEDF and this interaction stimulates the enzymatic phospholipase A_2 (PLA_2) activity of ATGL. Although ATGL plays an essential role for triglyceride catabolism in adipose tissue, liver, and muscles,[50–52] its role in neuronal tissues remains elusive. Because PLA_2 generates free fatty acid and lysophospholipids from membrane phospholipids and modulates neural cell functions including signal transduction and gene transcription,[53] the upstream mechanisms by which PEDF initiates the signaling cascade should be addressed in future studies.

The nuclear translocation of AIF has been shown to be involved in several types of neurodegeneration,[42,54,55] whereas AIF, which is embedded in the inner mitochondrial membrane, exerts a vital function in bioenergetic and redox metabolism in the healthy state.[17,18,56] The persistent down-regulation of its expression might not be feasible for neurons, because *Hq* mutant mice develop specific degeneration of neurons in the cerebellum and retina[17] and forebrain-specific AIF-null mice are embryonic lethal.[20] Therefore, the therapeutic approach using PEDF, which inhibits the AIF release, may be a reasonable strategy for retinal degeneration and other central nervous system diseases. Because the majority of RP diseases in human patients progress over several decades, the delay of the disease progression by PEDF may provide sufficient therapeutic benefits for patients with RP.

In conclusion, we have demonstrated that inhibition of the nuclear translocation of AIF is essential for the neuroprotective activity of PEDF in retinal degeneration. PEDF inhibits the AIF nuclear translocation via up-regulation of Bcl-2, leading to prevention of the photoreceptor apoptosis in RCS rats. These findings indicate that AIF is an essential effector molecule of photoreceptor apoptosis in inherited retinal degeneration, and that the blockade of the AIF release by PEDF may be a useful therapeutic strategy for retinal degenerative diseases such as RP.

Acknowledgments

We thank Drs. Eiji Akiba, Katsuyuki Mitomo, Toshiaki Tabata, and Makoto Inoue for their excellent technical assistance in vector construction and large-scale production; and Mr. Hiroshi Fujii, Miss Chie Arimatsu, and Fumie Doi for their assistance with the experiments.

References

1. Rebello G, Ramesar R, Vorster A, Roberts L, Ehrenreich L, Oppon E, Gama D, Bardien S, Greenberg J, Bonapace G, Waheed A, Shah GN, Sly WS: Apoptosis-inducing signal sequence mutation in carbonic anhydrase IV identified in patients with the RP17 form of retinitis pigmentosa. Proc Natl Acad Sci USA 2004, 101:6617–6622
2. Wang DY, Chan WM, Tam PO, Baum L, Lam DS, Chong KK, Fan BJ, Pang CP: Gene mutations in retinitis pigmentosa and their clinical implications. Clin Chim Acta 2005, 351:5–16
3. Portera-Cailliau C, Sung CH, Nathans J, Adler R: Apoptotic photoreceptor cell death in mouse models of retinitis pigmentosa. Proc Natl Acad Sci USA 1994, 91:974–978
4. Wong P: Apoptosis, retinitis pigmentosa, and degeneration. Biochem Cell Biol 1994, 72:489–498
5. Tombran-Tink J, Johnson LV: Neuronal differentiation of retinoblastoma cells induced by medium conditioned by human RPE cells. Invest Ophthalmol Vis Sci 1989, 30:1700–1707
6. Steele FR, Chader GJ, Johnson LV, Tombran-Tink J: Pigment epithelium-derived factor: neurotrophic activity and identification as a member of the serine protease inhibitor gene family. Proc Natl Acad Sci USA 1993, 90:1526–1530
7. Taniwaki T, Becerra SP, Chader GJ, Schwartz JP: Pigment epithelium-derived factor is a survival factor for cerebellar granule cells in culture. J Neurochem 1995, 64:2509–2517
8. Dawson DW, Volpert OV, Gillis P, Crawford SE, Xu H, Benedict W, Bouck NP: Pigment epithelium-derived factor: a potent inhibitor of angiogenesis. Science 1999, 285:245–248
9. Ogata N, Matsuoka M, Imaizumi M, Arichi M, Matsumura M: Decreased levels of pigment epithelium-derived factor in eyes with neuroretinal dystrophic diseases. Am J Ophthalmol 2004, 137:1129–1130
10. Ikeda Y, Goto Y, Yonemitsu Y, Miyazaki M, Sakamoto T, Ishibashi T, Tabata T, Ueda Y, Hasegawa M, Tobimatsu S, Sueishi K: Simian immunodeficiency virus-based lentivirus vector for retinal gene transfer: a preclinical safety study in adult rats. Gene Ther 2003, 10:1161–1169
11. Miyazaki M, Ikeda Y, Yonemitsu Y, Goto Y, Sakamoto T, Tabata T, Ueda Y, Hasegawa M, Tobimatsu S, Ishibashi T, Sueishi K: Simian lentiviral vector-mediated retinal gene transfer of pigment epithelium-derived factor protects retinal degeneration and electrical defect in Royal College of Surgeons rats. Gene Ther 2003, 10:1503–1511
12. Cayouette M, Smith SB, Becerra SP, Gravel C: Pigment epithelium-

derived factor delays the death of photoreceptors in mouse models of inherited retinal degenerations. Neurobiol Dis 1999, 6:523–532
13. Yabe T, Wilson D, Schwartz JP: NFkappaB activation is required for the neuroprotective effects of pigment epithelium-derived factor (PEDF) on cerebellar granule neurons. J Biol Chem 2001, 276:43313–43319
14. Stefanis L: Caspase-dependent and -independent neuronal death: two distinct pathways to neuronal injury. Neuroscientist 2005, 11:50–62
15. Susin SA, Lorenzo HK, Zamzami N, Marzo I, Snow BE, Brothers GM, Mangion J, Jacotot E, Costantini P, Loeffler M, Larochette N, Goodlett DR, Aebersold R, Siderovski DP, Penninger JM, Kroemer G: Molecular characterization of mitochondrial apoptosis-inducing factor. Nature 1999, 397:441–446
16. Susin SA, Daugas E, Ravagnan L, Samejima K, Zamzami N, Loeffler M, Costantini P, Ferri KF, Irinopoulou T, Prevost MC, Brothers G, Mak TW, Penninger J, Earnshaw WC, Kroemer G: Two distinct pathways leading to nuclear apoptosis. J Exp Med 2000, 192:571–580
17. Klein JA, Longo-Guess CM, Rossmann MP, Seburn KL, Hurd RE, Frankel WN, Bronson RT, Ackerman SL: The harlequin mouse mutation downregulates apoptosis-inducing factor. Nature 2002, 419:367–374
18. Vahsen N, Cande C, Briere JJ, Benit P, Joza N, Larochette N, Mastroberardino PG, Pequignot MO, Casares N, Lazar V, Feraud O, Debili N, Wissing S, Engelhardt S, Madeo F, Piacentini M, Penninger JM, Schagger H, Rustin P, Kroemer G: AIF deficiency compromises oxidative phosphorylation. EMBO J 2004, 23:4679–4689
19. Ye H, Cande C, Stephanou NC, Jiang S, Gurbuxani S, Larochette N, Daugas E, Garrido C, Kroemer G, Wu H: DNA binding is required for the apoptogenic action of apoptosis inducing factor. Nat Struct Biol 2002, 9:680–684
20. Cheung EC, Joza N, Steenaart NA, McClellan KA, Neuspiel M, McNamara S, MacLaurin JG, Rippstein P, Park DS, Shore GC, McBride HM, Penninger JM, Slack RS: Dissociating the dual roles of apoptosis-inducing factor in maintaining mitochondrial structure and apoptosis. EMBO J 2006, 25:4061–4073
21. Hisatomi T, Sakamoto T, Murata T, Yamanaka I, Oshima Y, Hata Y, Ishibashi T, Inomata H, Susin SA, Kroemer G: Relocalization of apoptosis-inducing factor in photoreceptor apoptosis induced by retinal detachment in vivo. Am J Pathol 2001, 158:1271–1278
22. Hisatomi T, Nakazawa T, Noda K, Almulki L, Miyahara S, Nakao S, Ito Y, She H, Kohno R, Michaud N, Ishibashi T, Hafezi-Moghadam A, Badley AD, Kroemer G, Miller JW: HIV protease inhibitors provide neuroprotection through inhibition of mitochondrial apoptosis in mice. J Clin Invest 2008, 118:2025–2038
23. Zhu C, Wang X, Huang Z, Qiu L, Xu F, Vahsen N, Nilsson M, Eriksson PS, Hagberg H, Culmsee C, Plesnila N, Kroemer G, Blomgren K: Apoptosis-inducing factor is a major contributor to neuronal loss induced by neonatal cerebral hypoxia-ischemia. Cell Death Differ 2007, 14:775–784
24. Stellmach V, Crawford SE, Zhou W, Bouck N: Prevention of ischemia-induced retinopathy by the natural ocular antiangiogenic agent pigment epithelium-derived factor. Proc Natl Acad Sci USA 2001, 98:2593–2597
25. Murakami Y, Ikeda Y, Yonemitsu Y, Tanaka S, Kondo H, Okano S, Kohno R, Miyazaki M, Inoue M, Hasegawa M, Ishibashi T, Sueishi K: Newly-developed Sendai virus vector for retinal gene transfer: reduction of innate immune response via deletion of all envelope-related genes. J Gene Med 2008, 10:165–176
26. Tsutsumi N, Yonemitsu Y, Shikada Y, Onimaru M, Tanii M, Okano S, Kaneko K, Hasegawa M, Hashizume M, Maehara Y, Sueishi K: Essential role of PDGFRalpha-p70S6K signaling in mesenchymal cells during therapeutic and tumor angiogenesis in vivo: role of PDGFRalpha during angiogenesis. Circ Res 2004, 94:1186–1194
27. Poot M, Zhang YZ, Kramer JA, Wells KS, Jones LJ, Hanzel DK, Lugade AG, Singer VL, Haugland RP: Analysis of mitochondrial morphology and function with novel fixable fluorescent stains. J Histochem Cytochem 1996, 44:1363–1372
28. Deshmukh M, Kuida K, Johnson EM Jr: Caspase inhibition extends the commitment to neuronal death beyond cytochrome c release to the point of mitochondrial depolarization. J Cell Biol 2000, 150:131–143
29. Seigel GM, Sun W, Wang J, Hershberger DH, Campbell LM, Salvi RJ: Neuronal gene expression and function in the growth-stimulated R28 retinal precursor cell line. Curr Eye Res 2004, 28:257–269
30. Ogata N, Nishikawa M, Nishimura T, Mitsuma Y, Matsumura M: Unbalanced vitreous levels of pigment epithelium-derived factor and vascular endothelial growth factor in diabetic retinopathy. Am J Ophthalmol 2002, 134:348–353
31. Duh EJ, Yang HS, Haller JA, De Juan E, Humayun MS, Gehlbach P, Melia M, Pieramici D, Harlan JB, Campochiaro PA, Zack DJ: Vitreous levels of pigment epithelium-derived factor and vascular endothelial growth factor: implications for ocular angiogenesis. Am J Ophthalmol 2004, 137:668–674
32. Notari L, Baladron V, Aroca-Aguilar JD, Balko N, Heredia R, Meyer C, Notario PM, Saravanamuthu S, Nueda ML, Sanchez-Sanchez F, Escribano J, Laborda J, Becerra SP: Identification of a lipase-linked cell membrane receptor for pigment epithelium-derived factor. J Biol Chem 2006, 281:38022–38037
33. Yu SW, Wang H, Poitras MF, Coombs C, Bowers WJ, Federoff HJ, Poirier GG, Dawson TM, Dawson VL: Mediation of poly(ADP-ribose) polymerase-1-dependent cell death by apoptosis-inducing factor. Science 2002, 297:259–263
34. Green DR, Kroemer G: The pathophysiology of mitochondrial cell death. Science 2004, 305:626–629
35. Yakovlev AG, Ota K, Wang G, Movsesyan V, Bao WL, Yoshihara K, Faden AI: Differential expression of apoptotic protease-activating factor-1 and caspase-3 genes and susceptibility to apoptosis during brain development and after traumatic brain injury. J Neurosci 2001, 21:7439–7446
36. Donovan M, Cotter TG: Caspase-independent photoreceptor apoptosis in vivo and differential expression of apoptotic protease activating factor-1 and caspase-3 during retinal development. Cell Death Differ 2002, 9:1220–1231
37. Wright KM, Linhoff MW, Potts PR, Deshmukh M: Decreased apoptosome activity with neuronal differentiation sets the threshold for strict IAP regulation of apoptosis. J Cell Biol 2004, 167:303–313
38. Segura MF, Sole C, Pascual M, Moubarak RS, Perez-Garcia MJ, Gozzelino R, Iglesias V, Badiola N, Bayascas JR, Llecha N, Rodriguez-Alvarez J, Soriano E, Yuste VJ, Comella JX: The long form of Fas apoptotic inhibitory molecule is expressed specifically in neurons and protects them against death receptor-triggered apoptosis. J Neurosci 2007, 27:11228–11241
39. Doonan F, Donovan M, Cotter TG: Caspase-independent photoreceptor apoptosis in mouse models of retinal degeneration. J Neurosci 2003, 23:5723–5731
40. Zeiss CJ, Neal J, Johnson EA: Caspase-3 in postnatal retinal development and degeneration. Invest Ophthalmol Vis Sci 2004, 45:964–970
41. Sanges D, Comitato A, Tammaro R, Marigo V: Apoptosis in retinal degeneration involves cross-talk between apoptosis-inducing factor (AIF) and caspase-12 and is blocked by calpain inhibitors. Proc Natl Acad Sci USA 2006, 103:17366–17371
42. Cheung EC, Melanson-Drapeau L, Cregan SP, Vanderluit JL, Ferguson KL, McIntosh WC, Park DS, Bennett SA, Slack RS: Apoptosis-inducing factor is a key factor in neuronal cell death propagated by BAX-dependent and BAX-independent mechanisms. J Neurosci 2005, 25:1324–1334
43. Muñoz-Pinedo C, Guio-Carrion A, Goldstein JC, Fitzgerald P, Newmeyer DD, Green DR: Different mitochondrial intermembrane space proteins are released during apoptosis in a manner that is coordinately initiated but can vary in duration. Proc Natl Acad Sci USA 2006, 103:11573–11578
44. Otera H, Ohsakaya S, Nagaura Z, Ishihara N, Mihara K: Export of mitochondrial AIF in response to proapoptotic stimuli depends on processing at the intermembrane space. EMBO J 2005, 24:1375–1386
45. Polster BM, Basanez G, Etxebarria A, Hardwick JM, Nicholls DG: Calpain I induces cleavage and release of apoptosis-inducing factor from isolated mitochondria. J Biol Chem 2005, 280:6447–6454
46. Yuste VJ, Moubarak RS, Delettre C, Bras M, Sancho P, Robert N, d'Alayer J, Susin SA: Cysteine protease inhibition prevents mitochondrial apoptosis-inducing factor (AIF) release. Cell Death Differ 2005, 12:1445–1448
47. Cao G, Xing J, Xiao X, Liou AK, Gao Y, Yin XM, Clark RS, Graham SH, Chen J: Critical role of calpain I in mitochondrial release of apoptosis-inducing factor in ischemic neuronal injury. J Neurosci 2007, 27:9278–9293

48. Yabe T, Kanemitsu K, Sanagi T, Schwartz JP, Yamada H: Pigment epithelium-derived factor induces pro-survival genes through cyclic AMP-responsive element binding protein and nuclear factor kappa B activation in rat cultured cerebellar granule cells: implication for its neuroprotective effect. Neuroscience 2005, 133:691–700
49. Modjtahedi N, Giordanetto F, Madeo F, Kroemer G: Apoptosis-inducing factor: vital and lethal. Trends Cell Biol 2006, 16:264–272
50. Zimmermann R, Strauss JG, Haemmerle G, Schoiswohl G, Birner-Gruenberger R, Riederer M, Lass A, Neuberger G, Eisenhaber F, Hermetter A, Zechner R: Fat mobilization in adipose tissue is promoted by adipose triglyceride lipase. Science 2004, 306:1383–1386
51. Haemmerle G, Lass A, Zimmermann R, Gorkiewicz G, Meyer C, Rozman J, Heldmaier G, Maier R, Theussl C, Eder S, Kratky D, Wagner EF, Klingenspor M, Hoefler G, Zechner R: Defective lipolysis and altered energy metabolism in mice lacking adipose triglyceride lipase. Science 2006, 312:734–737
52. Chung C, Doll JA, Gattu AK, Shugrue C, Cornwell M, Fitchev P, Crawford SE: Anti-angiogenic pigment epithelium-derived factor regulates hepatocyte triglyceride content through adipose triglyceride lipase (ATGL). J Hepatol 2008, 48:471–478
53. Farooqui AA, Horrocks LA: Brain phospholipases A2: a perspective on the history. Prostaglandins Leukot Essent Fatty Acids 2004, 71:161–169
54. Wang H, Shimoji M, Yu SW, Dawson TM, Dawson VL: Apoptosis inducing factor and PARP-mediated injury in the MPTP mouse model of Parkinson's disease. Ann NY Acad Sci 2003, 991:132–139
55. Culmsee C, Zhu C, Landshamer S, Becattini B, Wagner E, Pellecchia M, Blomgren K, Plesnila N: Apoptosis-inducing factor triggered by poly(ADP-ribose) polymerase and Bid mediates neuronal cell death after oxygen-glucose deprivation and focal cerebral ischemia. J Neurosci 2005, 25:10262–10272
56. Miramar MD, Costantini P, Ravagnan L, Saraiva LM, Haouzi D, Brothers G, Penninger JM, Peleato ML, Kroemer G, Susin SA: NADH oxidase activity of mitochondrial apoptosis-inducing factor. J Biol Chem 2001, 276:16391–16398